THE RELATION BETWEEN BLACK HOLE MASS AND HOST SPHEROID STELLAR MASS OUT TO $z \sim 2$

Vardha N. Bennert[1,4], Matthew W. Auger[1], Tommaso Treu[1,5], Jong-Hak Woo[2], and Matthew A. Malkan[3]
[1] Department of Physics, University of California, Santa Barbara, CA 93106, USA; vbennert@calpoly.edu, tt@physics.ucsb.edu, mauger@ast.cam.ac.uk
[2] Astronomy Program, Department of Physics and Astronomy, Seoul National University, Republic of Korea; woo@astro.snu.ac.kr
[3] Department of Physics and Astronomy, University of California, Los Angeles, CA 90095, USA; malkan@astro.ucla.edu

ABSTRACT

We combine *Hubble Space Telescope* images from the Great Observatories Origins Deep Survey with archival Very Large Telescope and Keck spectra of a sample of 11 X-ray-selected broad-line active galactic nuclei in the redshift range $1 < z < 2$ to study the black-hole-mass–stellar-mass relation out to a look-back time of 10 Gyr. Stellar masses of the spheroidal component ($M_{\mathrm{sph},\star}$) are derived from multi-filter surface photometry. Black hole masses (M_{BH}) are estimated from the width of the broad Mg II emission line and the 3000 Å nuclear luminosity. Comparing with a uniformly measured local sample and taking into account selection effects, we find evolution in the form $M_{\mathrm{BH}}/M_{\mathrm{sph},\star} \propto (1+z)^{1.96\pm0.55}$, in agreement with our earlier studies based on spheroid luminosity. However, this result is more accurate because it does not require a correction for luminosity evolution and therefore avoids the related and dominant systematic uncertainty. We also measure total stellar masses ($M_{\mathrm{host},\star}$). Combining our sample with data from the literature, we find $M_{\mathrm{BH}}/M_{\mathrm{host},\star} \propto (1+z)^{1.15\pm0.15}$, consistent with the hypothesis that black holes (in the range $M_{\mathrm{BH}} \sim 10^{8-9}\,M_\odot$) pre-date the formation of their host galaxies. Roughly, one-third of our objects reside in spiral galaxies; none of the host galaxies reveal signs of interaction or major merger activity. Combined with the slower evolution in host stellar masses compared to spheroid stellar masses, our results indicate that secular evolution or minor mergers play a non-negligible role in growing both BHs and spheroids.

Key words: accretion, accretion disks – black hole physics – galaxies: active – galaxies: evolution – quasars: general

Online-only material: color figures

1. INTRODUCTION

Active galactic nuclei (AGNs) are thought to represent an integral phase in the formation and evolution of galaxies during which the central supermassive black hole (BH) is growing through accretion. The empirical relations between BH mass (M_{BH}) and the properties of the host galaxy (e.g., Ferrarese & Merritt 2000; Gebhardt et al. 2000; Marconi & Hunt 2003; Häring & Rix 2004) have been explained by a combination of AGN feedback (e.g., Volonteri et al. 2003; Ciotti & Ostriker 2007; Di Matteo et al. 2008; Hopkins et al. 2009) and hierarchical assembly of M_{BH} and stellar mass through galaxy merging (e.g., Peng 2007; Jahnke & Maccio 2011).

The great interest in the origin of the scaling relations is reflected in the flood of observational studies, focusing on their cosmic evolution (e.g., Treu et al. 2004, 2007; Walter et al. 2004; Shields et al. 2006; McLure et al. 2006; Peng et al. 2006; Woo et al. 2006, 2008; Salviander et al. 2007; Jahnke et al. 2009; Bennert et al. 2010; Decarli et al. 2010; Merloni et al. 2010), with the majority pointing to a scenario in which BH growth precedes bulge assembly.

However, many high-redshift studies to date are based on monochromatic *Hubble Space Telescope* (*HST*) imaging, determining only the luminosity of the host spheroid and not its stellar mass. This is acceptable at $z \sim 0.5$ (e.g., Bennert et al. 2010), where the stellar populations of bulges are fairly well known and their luminosities can be passively evolved to zero redshift with uncertainties smaller than other sources of error. In contrast, at $z > 1$, the stellar populations of bulges are an uncharted

territory, particularly for AGN hosts which are believed to be connected with major mergers and may have undergone recent episodes of star formation (e.g., Kauffmann et al. 2003; Sánchez et al. 2004). The uncertainty on the conversion from observed luminosity to equivalent $z = 0$ luminosity can be comparable to the evolutionary signal (e.g., Peng et al. 2006).

An exception is the study by Merloni et al. (2010) who estimate total stellar masses ($M_{\mathrm{host},\star}$) and AGN luminosities by fitting spectral-energy distribution (SED) models to multi-band data from the rest-frame ultraviolet to the rest-frame mid-infrared for a sample of 89 broad-line AGN (BLAGN) hosts at $1 < z < 2.2$. Estimating M_{BH} from broad Mg II emission, they find that black holes of a given mass reside in less massive hosts at higher redshift with a modest evolutionary slope. However, Merloni et al. (2010) are unable to distinguish between $M_{\mathrm{host},\star}$ and the stellar mass of the central bulge component of the host ($M_{\mathrm{sph},\star}$). Such a difference may be important when studying the evolution of the scaling relations: there are indications that the relations between M_{BH} and *total host-galaxy* luminosity (Bennert et al. 2010) and stellar mass (Jahnke et al. 2009) may not be evolving, or at least not as rapidly as the relations between M_{BH} and *spheroid* properties.

In this paper, we study the cosmic evolution of the $M_{\mathrm{BH}}-M_{\mathrm{sph},\star}$ and $M_{\mathrm{BH}}-M_{\mathrm{host},\star}$ relations for a sample of 11 BLAGNs ($1 < z < 2$; look-back time: 8–10 Gyr) selected from the Great Observatories Origins Deep Survey (GOODS) fields, taking into account selection effects. $M_{\mathrm{sph},\star}$ and $M_{\mathrm{host},\star}$ are derived from the deep multi-filter *HST* images. M_{BH} is estimated using the width of the broad Mg II emission line, measured from existing spectra and the 3000 Å nuclear luminosity. We use a local comparison sample of Seyfert-1 galaxies (Bennert et al. 2011) for which all relevant quantities were derived following

---

[4] Current address: Physics Department, California Polytechnic State University, San Luis Obispo, CA 93407, USA.
[5] Packard Fellow.

Table 1
Sample Properties, BH Masses, and Stellar Masses

ID	R.A. (J2000)	Decl. (J2000)	z	Reference	$FWHM_{Mg\,II}$ (km s^{-1})	λL_{3000} (10^{44} erg s^{-1})	M_{BH}	$M_{sph,\star}$	$M_{disk,\star}$
(1)	(2)	(3)	(4)	(5)	(6)	(7)	(8)	(9)	(10)
J033252 − 275119	ID.88	ID.8	1.227	S10/S04	16208	0.43	9.01	9.83	10.50
J033243 − 274914	ID.24	ID.2	1.900	T09/S04	16381	1.77	9.31	10.64	. . .
J033239 − 274601	ID.09	ID.8	1.220	T09/S04	4344	5.38	8.39	10.54	. . .
J033226 − 274035	ID.50	ID.5	1.031	S10/S04	2430	9.51	8.00	9.53	10.75
J033225 − 274218	ID.17	ID.8	1.617	S10/S04	4744	1.64	8.22	10.61	. . .
J033210 − 274414	ID.91	ID.9	1.615	S10/S04	5852	2.02	8.45	10.45	. . .
J033200 − 274319	ID.36	ID.7	1.037	S10/L05	3602	1.08	7.90	9.62	. . .
J033229 − 274529	ID.98	ID.9	1.218	S10/M05	5308	4.33	8.52	10.71	. . .
J123553+621037	ID.13	ID.3	1.371	T08/W04	5441	2.32	8.41	9.99	10.84
J123618+621115	ID.58	ID.0	1.021	T08/W04	6988	1.19	8.49	9.29	10.95
J123707+622147	ID.46	ID.9	1.450	T08/W04	10654	1.57	8.91	10.74	. . .

Notes. Column 1: target ID (based on R.A. and decl.). Column 2: right ascension. Column 3: declination. Column 4: redshift (taken from Team Keck Redshift Survey (TKRS) (Wirth et al. 2004) for GOODS-N). Column 5: reference for catalog from which objects were selected/reference for origin of spectra. S10 = Silverman et al. (2010), T09 = Treister et al. (2009), T08 = Trouille et al. (2008); S04 = Szokoly et al. (2004), L05 = Le Févre et al. (2005), M05 = Mignoli et al. (2005), W04 = Wirth et al. (2004). Column 6: FWHM of broad Mg II. Column 7: rest-frame luminosity at 3000 Å (fiducial error 0.1 dex). Column 8: log $M_{BH}/M_\odot$ (uncertainty 0.5 dex). Column 9: stellar spheroid mass log $M_{sph,\star}/M_\odot$ (Chabrier IMF; uncertainty 0.3 dex for ellipticals, 0.4 dex for spirals). Column 10: stellar disk mass log $M_{disk,\star}/M_\odot$ (Chabrier IMF; uncertainty 0.3 dex).

the same procedures adopted for the distant sample to minimize potential systematic bias. Our strategy allows us to address two major limitations of previous studies: eliminate uncertainties due to luminosity evolution and determine the evolution of the spheroidal component of the host.

Throughout the paper, we assume a Hubble constant of $H_0 = 70$ km s^{-1} Mpc^{-1}, $\Omega_\Lambda = 0.7$, and $\Omega_M = 0.3$. Note that all magnitudes are AB.

2. DATA ANALYSIS

2.1. Sample Selection

The high-redshift sample consists of AGNs in GOODS-N (Treister et al. 2009) and GOODS-S (Trouille et al. 2008; Silverman et al. 2010), selected based on their X-ray emission using the Chandra Deep Field North and South (CDF-N/CDF-S) survey and spectroscopically confirmed to be BLAGNs. We select all 11 objects within $1 < z < 2$ for which archival Very Large Telescope (VLT) and Keck spectra covering the broad Mg II line exist (Table 1).

By design, all objects have deep *HST*/Advanced Camera for Surveys (ACS) images in four different broadband filters ($B =$ F435W, $V =$ F606W, $i =$ F775W, and $z =$ F850LP; Giavalisco et al. 2004). Color images are shown in Figure 1. The total exposure times range between 5000 and 25,000 s, depending on the filter and the image region. The reduced data are taken from the v2.0 data release.[6] The spatial resolution is approximately 0″.1 full width at half-maximum (FWHM), which at $z = 1.3$ (our average redshift) corresponds to 0.84 kpc; thus, our data have higher spatial resolution than Sloan Digital Sky Survey (SDSS) images at $z = 0.05$ (1″.4 = 1.37 kpc). Overall, the AGN host galaxies look like typical ellipticals or spirals, without any signs of merger activity.

Our local comparison sample consists of 25 Seyfert-1 galaxies selected from SDSS ($0.02 < z < 0.1$; $M_{BH} > 10^7 M_\odot$) for which all relevant quantities were derived following the same

procedures adopted for the distant sample to minimize potential systematic bias (Bennert et al. 2011).

2.2. Surface Photometry

We perform two-dimensional surface photometry using the code "Surface Photometry and Structural Modeling of Imaging Data" developed by one of us (M.W.A.). The code allows a joint multi-band analysis of surface brightness models, thus superceding the functionality of GALFIT (Peng et al. 2002), and is described in detail in Bennert et al. (2011). The point-spread function (PSF) of the *HST*/ACS optics is modeled using the closest bright star to a given object. We impose a Gaussian prior on the AGN colors with the mean given by the quasar composite spectrum from Vanden Berk et al. (2001) redshifted to the AGN redshift and with a σ of 0.2 mag. We model the host galaxy by either a single de Vaucouleurs (1948) profile or by a de Vaucouleurs (1948) profile plus an exponential profile to account for a disk. Depending on the images and residuals, we decide whether a given object is best fitted by three components (PSF, spheroid, and disk) or two components (PSF + spheroid), as described by Treu et al. (2007) and Bennert et al. (2010, 2011). A disk component is evident in 4/11 objects. In all four cases, we can only clearly detect the bulge in the z band.

To probe the reliability of our AGN-host-galaxy decompositions when using the blue rest-frame wavelengths covered by the GOODS images, we tested the effect of bandpass shifting. Given the host-galaxy morphology and level of activity of the sample studied here, a local sample of Seyfert galaxies is a suitable comparison sample for this test. (Schawinski et al. 2011 also concluded that "moderate luminosity AGN host galaxies at $z \simeq 2$ and $z \simeq 0$ are remarkably similar.") We thus repeated the analysis of our local sample of AGN host galaxies (Bennert et al. 2011), but now using only *ug* SDSS photometry (instead of *griz*). We are able to recover the photometry of the bulge and point source to within 0.1 mag, i.e., smaller than our adopted systematic uncertainty, demonstrating that bandpass shifting is not a concern within our level of precision. Moreover, this is a conservative estimation, since the GOODS images at $z \simeq 1.3$ not only cover wavelengths comparable to *ug* rest frame (F775W

---

6 http://archive.stsci.edu/pub/hlsp/goods/v2/
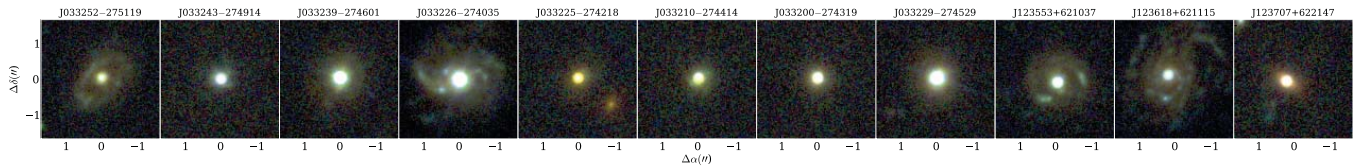
Figure 1. Deep *HST*/ACS color images (*B, V, i, z*), $3'' \times 3''$.
(A color version of this figure is available in the online journal.)

Table 2
Results from Surface Photometry

Object	PSF				Spheroid				Disk			
	B	*V*	*i*	*z*	*B*	*V*	*i*	*z*	*B*	*V*	*i*	*z*
	(mag)	(mag)	(mag)	(mag)	(mag)	(mag)	(mag)	(mag)	(mag)	(mag)	(mag)	(mag)
(1)	(2)	(3)	(4)	(5)	(6)	(7)	(8)	(9)	(10)	(11)	(12)	(13)
J033252 − 275119	25.03	23.84	23.40	23.47	. . .	. . .	. . .	23.86	24.12	23.49	22.84	22.18
J033243 − 274914	22.53	23.09	22.98	23.10	25.30	24.68	23.67	23.37	. . .	. . .	. . .	. . .
J033239 − 274601	21.33	21.08	21.14	21.38	24.17	24.32	23.06	22.10	. . .	. . .	. . .	. . .
J033226 − 274035	20.26	20.04	20.04	20.01	. . .	. . .	. . .	23.27	22.22	21.87	21.22	20.63
J033225 − 274218	25.38	23.87	22.84	22.50	25.08	24.61	23.84	23.08	. . .	. . .	. . .	. . .
J033210 − 274414	24.24	23.19	22.61	22.74	24.13	24.10	23.55	22.96	. . .	. . .	. . .	. . .
J033200 − 274319	22.81	22.42	22.45	22.47	43.90	25.33	24.00	23.04	. . .	. . .	. . .	. . .
J033229 − 274529	21.24	21.31	21.42	21.76	23.80	23.32	22.49	21.66	. . .	. . .	. . .	. . .
J123553+621037	22.55	22.12	22.15	22.33	. . .	. . .	. . .	24.04	23.62	23.20	22.45	21.83
J123618+621115	22.77	22.27	22.62	22.81	. . .	. . .	. . .	23.87	23.15	22.37	21.40	20.79
J123707+622147	23.16	22.97	22.69	22.55	24.95	24.66	23.46	22.57	. . .	. . .	. . .	. . .

Notes. Column 1: target ID. Columns 2–5: extinction-corrected *B, V, i,* and *z* PSF magnitudes (uncertainty 0.2 mag). Columns 6–9: extinction-corrected *B, V, i,* and *z* spheroid magnitudes (uncertainty 0.2 mag). Columns 10–13: extinction-corrected *B, V, i,* and *z* disk magnitudes (uncertainty 0.2 mag).

and F850LP), but additionally also shorter wavelengths (F606W and F435W), thus effectively providing more information to disentangle point source and bulge. Furthermore, as already pointed out above, the GOODS images of $z \gtrsim 1.3$ objects have even higher resolution than SDSS images at ~ 0.5.

2.3. Stellar Mass

From the resulting magnitudes (Table 2), stellar masses are estimated using a Bayesian stellar-mass estimation code (Auger et al. 2009) assuming a Chabrier initial mass function (IMF; Table 1). We impose conservative uncertainties of 0.3 dex on the masses of the bulges (disks) for the bulge-dominated (disk-dominated) hosts. The masses for the bulge components of the disk-dominated hosts are estimated by using the *z*-band mass-to-light ratios of the bulge-dominated hosts in our sample that are at similar redshifts; we therefore add in quadrature a 0.3 dex uncertainty, yielding a total stellar mass uncertainty of 0.4 dex for these objects. For two of our objects, Schawinski et al. (2011) report stellar masses based upon template fits to the integrated light. Our results agree within the uncertainties (assumed to be 0.2 dex for Schawinski et al. 2011).

2.4. BH Mass

Black hole masses are estimated via the empirically calibrated photoionization method ("virial method") (e.g., Wandel et al. 1999; Vestergaard & Peterson 2006; McGill et al. 2008), by combining the FWHM of the broad Mg II λ2798 Å emission line and the 3000 Å AGN continuum luminosity

(McGill et al. 2008):

$$\log M_{BH} = 6.767 + 2 \log \left(\frac{\text{FWHM}_{\text{Mg II}}}{1000 \, \text{km s}^{-1}} \right) + 0.47 \log \left(\frac{\lambda L_{3000}}{10^{44} \, \text{erg s}^{-1}} \right).$$

The AGN luminosity is derived from the PSF magnitudes in the filter closest to rest-frame 3000 Å and extrapolated based on the assumed AGN SED of Vanden Berk et al. (2001) (Section 2.2; Table 1).

The nominal uncertainty of M_{BH} using this method is 0.4 dex. However, for some spectra, the low signal-to-noise makes the FWHM measurements uncertain by up to ∼50%, conservatively estimated. Moreover, the spectra are not of sufficient quality to remove the Fe emission which can result in overestimating the width of Mg II by up to 0.03 dex (in FWHM; McGill et al. 2008; see, however, Merloni et al. 2010). We therefore adopt an uncertainty of 0.5 dex. Note that while we used uniform priors for both the 3000 Å luminosity and the black hole mass in our analysis, employing more informed priors from the quasar luminosity function of Richards et al. (2006) or the black hole mass function of Kelly et al. (2010) yield negligible changes to our inference.

2.5. M_{BH}–$M_{\star}$ Evolution

Following and expanding on work by Treu et al. (2007) and Bennert et al. (2010), we model the evolution of the offset of the M_{BH}–$M_{sph,\star}$ and M_{BH}–$M_{host,\star}$ scaling relations by assuming a model of the form

$$\log M_{BH} - 8 = \alpha[\log M_* - 10] + \beta \log [1 + z] + \gamma + \sigma,$$
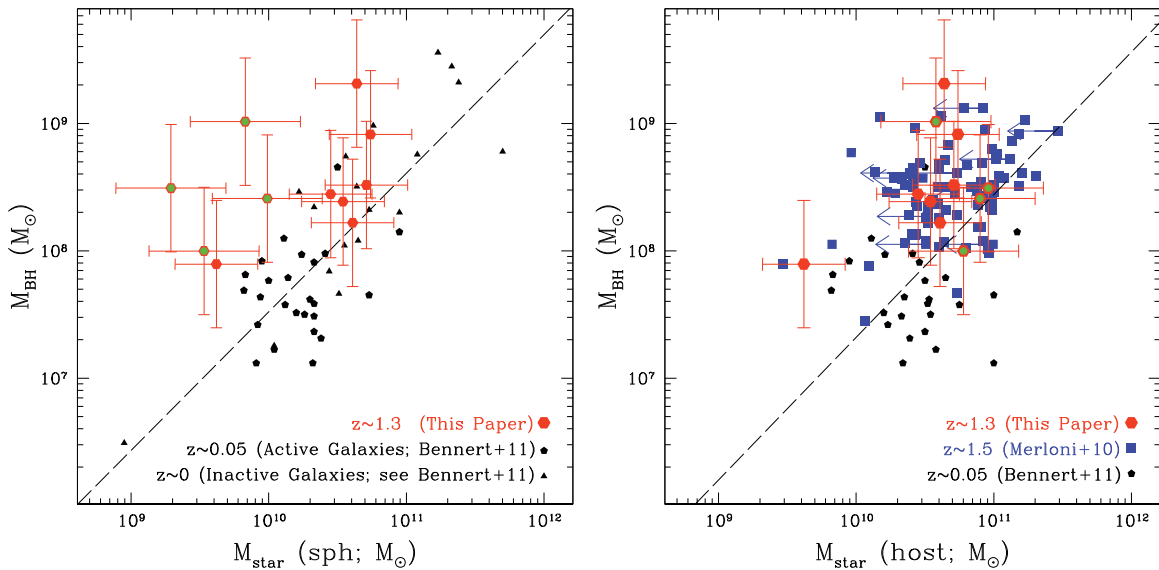
Figure 2. Left panel: M_{BH}–$M_{sph,\star}$ relation for our sample (red pentagons; green circles if fitted by spheroid plus disk), local BLAGNs (black circles; Bennert et al. 2011), and local inactive galaxies (black triangles; Bennert et al. 2011), with the $z = 0$ relation (see Section 2.5). The errors for the local samples are omitted for clarity (0.4 dex in M_{BH} and 0.25 dex in $M_{sph,\star}$). Right panel: the same as in the left panel for total host-galaxy stellar mass. Here, we overplot the 89 BLAGNs from Merloni et al. (2010) (blue filled squares; 10 with upper limits indicated by arrows).

(A color version of this figure is available in the online journal.)

where α is the slope of the relations at $z = 0$ and is assumed not to evolve, γ is the intercept of the relations at $z = 0$, and σ is the intrinsic scatter which is also assumed to be non-evolving. Here β describes the evolution of the scaling relation (with $\beta = 0$ implying no evolution). We impose δ-function priors of $\alpha = 1.09$ (Bennert et al. 2011) and $\gamma = -0.48$ for the $M_{sph,*}$ relation and $\alpha = 1.12$ (Häring & Rix 2004) and $\gamma = -0.68$ for the $M_{Host,*}$ relation; the priors on γ were determined by fitting to the local AGNs from Bennert et al. (2011) while keeping the slope fixed to the noted values. A normal distribution prior is used for the intrinsic scatter with mean 0.4 and variance 0.01 and we employ a broad uniform prior for β. (Note that, strictly speaking, the variable σ accounts for both the intrinsic scatter in the relationship and the (much smaller) uncertainty on γ.) We use the $z = 1.0$–1.2 "elliptical" stellar mass function from Ilbert et al. (2010) to place priors on the stellar masses. Furthermore, we include a prior on the black hole masses that models our selection effects by using a hard cutoff at the low-mass end. This cutoff is determined from the data and models the lower limit of black hole masses observable in each set of data considered.

The relation above is first fitted using the 11 galaxies in this sample. The lower limit for the black hole masses assumed for the high-redshift objects is $10^{7.4} M_\odot$. Merloni et al. (2010) have independently tried to infer the evolution of the M_{BH}–$M_{host,\star}$ relation, but their analysis is somewhat different than ours (e.g., IMFs, local comparison samples, definition of offset, treatment of upper limits, and selection effects). We therefore also fit the relation using the Merloni et al. (2010) data (adjusted to a Chabrier IMF), and we impose a limiting black hole mass of $10^{7.3}$ for these data. The results of our inference are shown in Table 3. Given that the different fits to the M_{BH}–$M_{host,\star}$ relation (Merloni et al. data only, our data only, both combined) result in the same β within the uncertainties, we adopt the one for the combined sample in the following.

3. RESULTS AND DISCUSSION

Out of 11, four AGNs are clearly hosted by late-type spiral galaxies, while the rest seem to be spheroid dominated.

Table 3
Evolving M_{BH}–M_* Scaling Relations

| Model	α	β	γ	σ
$M_{sph,*}$ [a]	1.09	1.96 ± 0.55	-0.48	0.36 ± 0.1
$M_{host,*}$ [a]	1.12	1.68 ± 0.53	-0.68	0.35 ± 0.1
$M_{host,*}$ [b]	1.12	1.15 ± 0.15	-0.68	0.16 ± 0.06
$M_{host,*}$ [c]	1.12	1.11 ± 0.16	-0.68	0.17 ± 0.07

Notes.
[a] Fitted only using the 11 objects presented here.
[b] Fitted using the objects presented here and the objects from Merloni et al. (2010).
[c] Fitted only using data from Merloni et al. (2010).

Keeping in mind the small number statistics, the fraction of disk-dominated host galaxies ($36\% \pm 17\%$) is lower than what has been found by Schawinski et al. (2011) ($80\% \pm 10\%$) for 20 X-ray-selected AGNs at a comparable redshift ($1.5 < z < 3$) imaged by *HST*/Wide Field Camera 3 (F160W) with 1–2 orbits integration time. One difference is that our objects have higher X-ray luminosities (0.5–8 keV; $43.5 < \log L_X < 44.5$, mean $= 44.2$, compared to $42 < \log L_X < 44$, mean $= 43.1$) which might explain why we find a larger fraction of elliptical host galaxies.

Interestingly, none of the objects shows clear signs of interactions or merger activity, while at redshifts of $z = 0.4$–0.6, $32\% \pm 9\%$ of Seyfert-1s are hosted by interacting/merging galaxies (Bennert et al. 2010). However, we cannot exclude that some of these low surface brightness features might have been missed (see, e.g., Bennert et al. 2008). Schawinski et al. (2011) also do not report interactions/mergers but their images are significantly shallower than ours. Star-forming galaxies at a redshift of $z \sim 2$, on the other hand, show a $33\% \pm 6\%$ fraction of interacting or merging systems (Förster-Schreiber et al. 2009). Schawinski et al. (2011) interpret their high fraction of spiral galaxies as a sign that secular evolution may play a non-negligible role in growing spheroids and black holes. Our
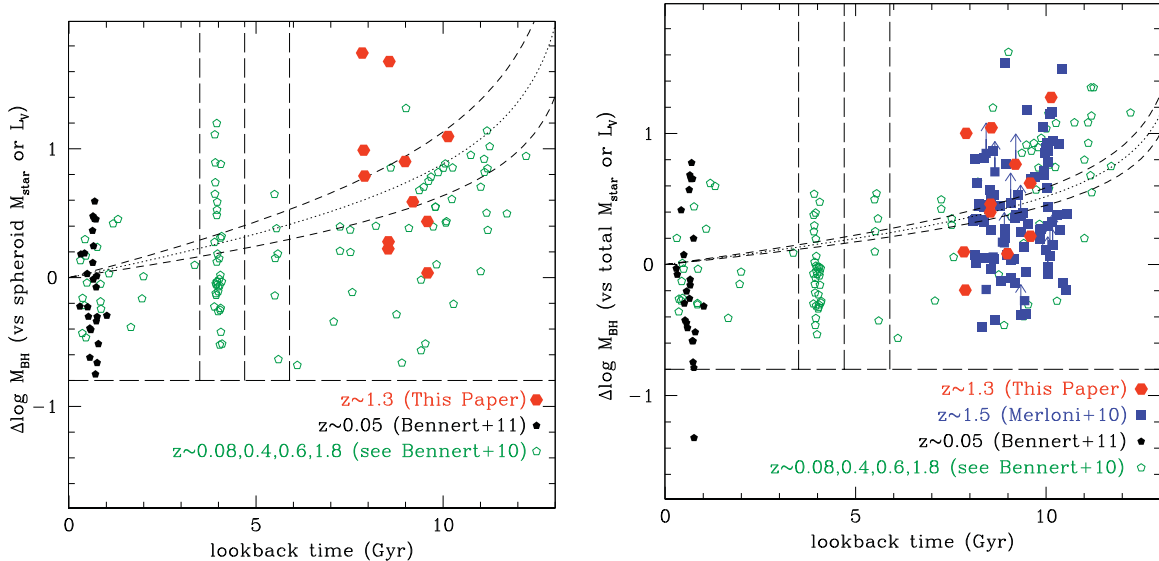
Figure 3. Left panel: offset in log M_{BH} as a function of constant $M_{sph,\star}$ (our objects: red filled pentagons) with respect to the fiducial local relation of AGNs (black filled circles). The offset in log M_{BH} as a function of constant stellar spheroid luminosity from Bennert et al. (2010) is overplotted (green open symbols), corresponding to AGNs at different redshifts, (left to right: z 0.08, reverberation-mapped AGN from Bennert et al. 2010; Bentz et al. 2009; z 0.4 from Bennert et al. 2010; Treu et al. 2007; z 0.6 from Bennert et al. 2010; z 1.8 from Bennert et al. 2010; Peng et al. 2006). The best linear fit derived here is overplotted as a dotted line ($M_{BH}/M_{sph,\star} \propto (1+z)^{1.96\pm0.55}$; dashed lines: 1σ range). Right panel: the same as in the left panel as an offset in log M_{BH} as a function of constant total host-galaxy mass (luminosity for Bennert et al. 2010). The Merloni et al. (2010) sample is overplotted (blue filled squares). The lines correspond to $M_{BH}/M_{host,\star} \propto (1+z)^{1.15\pm0.15}$. (A color version of this figure is available in the online journal.)

findings, including the lack of merger activity, are consistent with such a scenario.

Figure 2 (left) shows the $M_{BH}-M_{sph,\star}$ relation, including a sample of 18 inactive galaxies and the local AGNs from Bennert et al. (2011). In Figure 2 (right), we show the $M_{BH}-M_{host,\star}$ relation, again including the local AGNs from Bennert et al. (2011) and additionally the 89 AGNs from Merloni et al. (2010) (10/89 with upper limits only; subtracting 0.255 dex to convert their total stellar masses from Salpeter to Chabrier IMF, Bruzual & Charlot 2003). Note that for all comparison samples, M_{BH} were estimated using the same recipe adopted here.

In Figure 3, we show the offset in log M_{BH} as a function of constant $M_{sph,\star}$ (left panel) and $M_{host,\star}$ (right panel) with respect to the $z = 0$ relations (see Section 2.5). For comparison, the offset in log M_{BH} as a function of constant stellar spheroid luminosity (left panel) and total luminosity (right panel) from Bennert et al. (2010) is overplotted. Taking into account selection effects (Section 2.5), we find significant evolution in $M_{BH}/M_{sph,\star}$ ($\propto (1+z)^{1.96\pm0.55}$), consistent with (but with larger uncertainties) what we reported previously for the evolution of the $M_{BH}-L_{sph}$ relation ($M_{BH}/L_{sph} \propto (1+z)^{1.4\pm0.2}$; Bennert et al. 2010). The agreement between the stellar mass and luminosity evolution suggests that the passive luminosity correction is appropriate, although modeling luminosity evolution rather than stellar masses may increase the scatter.

For total stellar masses, including the Merloni et al. (2010) data, the evolutionary trend can be described as $M_{BH}/M_{host,\star} \propto (1+z)^{1.15\pm0.15}$, in agreement with what has been found by Merloni et al. (2010) within the uncertainties. This evolution is slower than the one for spheroid masses ($\beta = 1.96 \pm 0.55$) in line with recent studies (Jahnke et al. 2009; Bennert et al. 2010). It indicates that the amount by which at least some of the distant AGN host galaxies have to grow their bulge component in order to fall on the local BH mass scaling relations is contained within the galaxy itself. It can thus be considered as further evidence that secular evolution and/or

minor mergers play a non-negligible role in growing spheroids through a redistribution of stars from disk to bulge. The deduced evolution is either in line with or slightly faster than what has been predicted by theoretical studies (for a detailed comparison, see, e.g., Bennert et al. 2010; Lamastra et al. 2010).

4. CONCLUSIONS

We determine spheroid and total stellar masses for the host galaxies of 11 X-ray-selected BLAGNs ($1 < z < 2$) in GOODS. In combination with M_{BH} estimated via the virial method from the broad Mg II emission line as measured from archival VLT and Keck spectra and the 3000 Å nuclear luminosity, we study the evolution of the $M_{BH}-M_\star$ scaling relation out to a look-back time of 10 Gyr. Using a uniformly measured local comparison sample and taking into account selection effects, we find evolution of the correlations consistent with BH growth preceding galaxy assembly, confirming and extending the results of previous studies (e.g., Merloni et al. 2010; Decarli et al. 2010; Bennert et al. 2010).

Our results show that a significant fraction (4/11) of AGNs at $z = 1$–2 are hosted by spiral galaxies. None of the galaxies show evidence for recent major merger interaction, contrary to the general assumption that BHs and spheroids grow predominantly through major mergers, a scenario which might hold true only for the most luminous AGNs. The evolution we find for the M_{BH}–total-stellar-mass relation is slower than the one for spheroid stellar masses in line with recent studies (Jahnke et al. 2009; Bennert et al. 2010). Combined, our results indicate that secular evolution and/or minor mergers play a non-negligible role in growing both BHs and spheroids.

Our study demonstrates the feasibility of obtaining stellar masses of AGN host galaxies out to look-back times of 10 Gyr based on deep multicolor *HST* photometry. This approach has the great advantage of being independent of the luminosity evolution correction—the dominant source of systematic

uncertainty in previous studies at comparable redshifts (e.g., Peng et al. 2006; Bennert et al. 2010). Furthermore, we can distinguish between spheroid and total host-galaxy mass, which is not possible based on SED fitting (e.g., Merloni et al. 2010).

Sample size is a major limitation of this work, allowing us to constrain only average evolution and preventing us from investigating, e.g., mass-dependent trends or correlations between evolution and morphology. Follow-up of BLAGN hosts imaged by existing and upcoming multicolor *HST* surveys (e.g., CANDLES) is needed to gather larger samples and address these remaining issues.

REFERENCES

Auger, M. W., Treu, T., Bolton, A. S., et al. 2009, ApJ, 705, 1099
Bennert, N., Canalizo, G., Jungwiert, B., et al. 2008, ApJ, 677, 846
Bennert, V. N., Auger, M. W., Treu, T., Woo, J.-H., & Malkan, M. A. 2011, ApJ, 726, 59
Bennert, V. N., Treu, T., Woo, J.-H., et al. 2010, ApJ, 708, 1507
Bentz, M. C., Peterson, B. M., Pogge, R. W., & Vestergaard, M. 2009, ApJ, 694, 166
Bruzual, G., & Charlot, S. 2003, MNRAS, 344, 1000
Ciotti, L., & Ostriker, J. P. 2007, ApJ, 665, L5
Decarli, R., Falomo, R., Treves, A., et al. 2010, MNRAS, 402, 2453
de Vaucouleurs, G. 1948, Ann. d'Astrophys., 11, 247

Di Matteo, T., Colberg, J., Springel, V., Hernquist, L., & Sijacki, D. 2008, ApJ, 676, 33
Ferrarese, L., & Merritt, D. 2000, ApJ, 539, L9
Förster-Schreiber, N., Genzel, R., Bouché, N., et al. 2009, ApJ, 706, 1364
Gebhardt, K., Bender, R., Bower, G., et al. 2000, ApJ, 539, L13
Giavalisco, M., Ferguson, H. C., Koekemoer, A. M., et al. 2004, ApJ, 600, 93
Häring, N., & Rix, H.-W. 2004, ApJ, 604, L89
Hopkins, P. F., Murray, N., & Thompson, T. A. 2009, MNRAS, 398, 303
Ilbert, O., Salvato, M., Le Floc'h, E., et al. 2010, ApJ, 709, 644
Jahnke, K., Bongiorno, A., Brusa, M., et al. 2009, ApJ, 706, 215
Jahnke, K., & Maccio, A. 2011, ApJ, 734, 92
Kauffmann, G., Heckman, T. M., Tremonti, C., et al. 2003, MNRAS, 346, 1055
Kelly, B., Vestergaard, M., Fan, X., et al. 2010, ApJ, 719, 1315
Lamastra, A., Menci, N., Maiolino, R., Fiore, F., & Merloni, A. 2010, MNRAS, 405, 29
Le Févre, O., Vettolani, G., Garilli, B., et al. 2005, A&A, 439, 845
Marconi, A., & Hunt, L. K. 2003, ApJ, 589, L21
McGill, K. L., Woo, J.-H., Treu, T., & Malkan, M. A. 2008, ApJ, 673, 703
McLure, R. J., Jarvis, M. J., Targett, T. A., Dunlop, J. S., & Best, P. N. 2006, MNRAS, 368, 1395
Merloni, A., Bongiorno, A., Bolzonella, M., et al. 2010, ApJ, 708, 137
Mignoli, M., Cimatti, A., Zamorani, G., et al. 2005, A&A, 437, 883
Peng, C. Y. 2007, ApJ, 671, 1098
Peng, C. Y., Ho, L. C., Impey, C. D., & Rix, H.-W. 2002, AJ, 124, 266
Peng, C. Y., Impey, C. D., Rix, H.-W., et al. 2006, ApJ, 649, 616
Richards, G. T., Strauss, M. A., Fan, X., et al. 2006, AJ, 131, 2766
Salviander, S., Shields, G. A., Gebhardt, K., & Bonning, E. W. 2007, ApJ, 662, 131
Sánchez, S. F., Jahnke, K., Wisotzki, L., et al. 2004, ApJ, 614, 586
Schawinski, K., Treister, E., Urry, C. M., et al. 2011, ApJ, 727, L31
Shields, G. A., Menezes, K. L., Massart, C. A., & Vanden Bout, P. 2006, ApJ, 641, 683
Silverman, J. D., Mainieri, V., Salvato, M., et al. 2010, ApJS, 191, 124
Szokoly, G. P., Bergeron, J., Hasinger, G., et al. 2004, ApJS, 155, 271
Treister, E., Virani, S., Gawiser, E., et al. 2009, ApJ, 693, 1713
Treu, T., Malkan, M. A., & Blanford, R. D. 2004, ApJ, 615, L97
Treu, T., Woo, J.-H., Malkan, M. A., & Blanford, R. D. 2007, ApJ, 667, 117
Trouille, L., Barger, A. J., Cowie, L. L., Yang, Y., & Mushotzky, R. F. 2008, ApJS, 179, 1
Vanden Berk, D. E., Richards, G. T., Bauer, A., et al. 2001, AJ, 122, 549
Vestergaard, M., & Peterson, B. M. 2006, ApJ, 641, 689
Volonteri, M., Haardt, F., & Madau, P. 2003, ApJ, 582, 559
Walter, F., Carilli, C., Bertoldi, F., et al. 2004, ApJ, 615, L17
Wandel, A., Peterson, B. M., & Malkan, M. A. 1999, ApJ, 526, 579
Wirth, G. D., Willmer, C. N. A., Amico, P., et al. 2004, AJ, 127, 3121
Woo, J.-H., Treu, T., Malkan, M. A., & Blandford, R. D. 2006, ApJ, 645, 900
Woo, J.-H., Treu, T., Malkan, M. A., & Blandford, R. D. 2008, ApJ, 681, 925